

# Search for giant pulses of radio pulsars at frequency 111 MHz with LPA radio telescope

Andrey Nikolaevich Kazantsev and Vladimir Alexeevich Potapov

P. N. Lebedev Physical Institute of the Russian Academy of Sciences, Pushchino Radio Astronomy Observatory, Pushchino 142290, Russia; [kaz.prao@bk.ru](mailto:kaz.prao@bk.ru)

Received 2017 December 5; accepted 2018 February 13

**Abstract** We have used the unique low frequency sensitivity of the Large Phased Array (LPA) radio telescope of Pushchino Radio Astronomy Observatory to collect a dataset consisting of single pulse observations of second period pulsars in the Northern Hemisphere. During observation sessions in 2011–2017, we collected data on 71 pulsars at a frequency of 111 MHz using a digital pulsar receiver. We have discovered Giant Radio Pulses (GRPs) from pulsars B0301+09 and B1237+25, and confirmed earlier reported generation of anomalously strong (probable giant) pulses from B1133+16 in a statistically significant dataset. Data for these pulsars and from B0950+08 and B1112+50, earlier reported as pulsars generating GRPs, were analyzed to evaluate their behavior over long time intervals. It was found that the statistical criterion (power-law spectrum of GRP distribution of energy and peak flux density) seems not to be strict for pulsars with a low magnetic field at their light cylinder. Moreover, spectra of some of these pulsars demonstrate unstable behavior with time and have a complex multicomponent shape. In the dataset for B0950+08, we have detected the strongest GRP from a pulsar with a low magnetic field at its light cylinder ever reported, having a peak flux density as strong as 16.8 kJy.

**Key words:** stars: neutron — pulsars: general — pulsars: individual (PSR B0301+19, PSR B0320+39, PSR B0329+54, PSR B0809+74, PSR B0950+08, PSR B1112+50, PSR B1133+16, PSR B1237+25) — pulsars: giant pulses, individual pulses

## 1 INTRODUCTION

Typical radio pulsars have very stable average pulse profiles, obtained from summing a sequence of thousands of individual pulses. At the same time, individual pulses emitted by a neutron star are very unstable both due to instability in the process of pulse emission and to effects of the perturbation on the interstellar medium. Individual pulses may be observed for only about one third of known radio pulsars because of their low flux density. Individual pulses can differ essentially from each other in terms of shape, duration and intensity (energy and peak flux density). When shape and duration of individual pulses may change in quite wide limits, fluctuation of intensity can reach extraordinary values. A strong fluctuation of intensity was noticed in an early work about the pulsar in the Crab Nebula (Staelin & Reifenstein 1968). An accurate analysis of the Crab pulsar at 160 MHz was

carried out in Sutton et al. (1971). It was shown that the Crab pulsar regularly generates very strong individual pulses, and the intensity distribution of pulses exhibits a bimodal form: log-normal distribution for quite weak (regular) pulses and power-law distribution for strong pulses. Strong pulses which exceed the average pulse by more than 30 times in intensity were called Giant Radio Pulses (GRPs). The statistical criterion (power-law form of intensity distribution) became one of the most important aspects for classification of GRPs. For a long time, the Crab pulsar was the only known pulsar emitting GRPs. Later on, GRPs from the fastest known (at the time) millisecond pulsar, B1937+21, were identified (Wolszczan et al. 1984, Cognard et al. 1996). After many years, similar phenomena were found from a set of pulsars (Singal 2001; Romani & Johnston 2001; Ershov & Kuzmin 2003; Joshi et al. 2004; Kuzmin et al. 2004; Joshi et al. 2004; Knight et al. 2005; Kuzmin & Ershov

2006; Ershov & Kuzmin 2006). Discovery of GRPs from pulsars outside of our Galaxy was reported for two pulsars in the Large Magellanic Cloud (LMC, Johnston & Romani 2003; Crawford et al. 2013).

The list of criteria for identifying giant pulses was compiled over time and contains the following items:

- GRP peak flux density is 30 times or more stronger and the energy in an individual pulse is more than 10 times as strong as those of an average pulse;
- GRPs are localized at longitude of average pulse profile or interpulse;
- peak flux density is on the order of hundreds or thousands of (in the case of the Crab pulsar, even millions of) Jy;
- short duration of a GRP in comparison with an average pulse and an extremely short duration if it has microstructure components (up to 0.4 ns for the Crab pulsar Hankins & Eilek 2007);
- a high level of linear and circular polarization in the GRP;
- power-law peak flux density and energy in the pulse distribution;
- extremely high brightness temperature for narrower pulses, up to about  $10^{41}$  K for the Crab pulsar (Hankins & Eilek 2007).

Not all items listed above are necessarily present at the same time for all GRPs. Sometimes this aspect makes a strict definition of a GRP tricky. A statistical criterion (connected with the type of distribution) is mostly taken as crucial, but, as will be shown below, this criterion seems to be not as robust as was thought previously, at least for second period pulsars with a low magnetic field at their light cylinder.

It is worth noting that generation of strong pulses, more than 30 times larger than average, is very rare for the vast majority of pulsars. Such a phenomenon is mostly connected with the far right “tail” of the log-normal distribution in flux (Taylor & Huguenin 1971; Hesse & Wielebinski 1974; Ritchings 1976).

It is easy to see that the pulsars listed in Table 1 can be divided into two subclasses:

- Pulsars with strong (over  $B_{LC} > 10^5$  G) magnetic fields at their light cylinders and millisecond period of rotation that can be observed at frequencies above 600 MHz. The most typical pulsars in this subclass are B0531+21, the Crab Nebula pulsar and the rapid millisecond pulsar B1937+21, which were observed over a wide range of frequencies. Their pulses

demonstrate submicrosecond sub-structure and extremely high peak flux density up to millions of Jy.

- Pulsars with  $B_{LC}$  from several to several hundred Gauss. These are pulsars have second periods and have been observed only at frequencies 40–111 MHz (with the only exception being J0529–6652). Their GRPs are as strong as several hundred or thousands of Jy, and exceed the average profiles by factors of tens, and their widths are of the same order as the average profile.

The problem of developing an adequate theoretical description of the phenomenon of GRP generation must take into account a wide range of parameters describing a pulsar with GRPs. The list of such pulsars includes both millisecond pulsars and second period pulsars, both pulsars with weak and strong magnetic fields at light cylinder, and young active pulsars (such as the Crab pulsar) and old recycled pulsars (such as B1937+21). Up to now, no single theoretical model has been developed which can predict emission of GRPs by using a function of known pulsar parameters. The majority of existing models is related to describing so called “classical” pulsars with GRPs (B0531+21, Crab pulsar and B1937+21) (Petrova 2006). The existing deficit in observed data on second period pulsars with a low magnetic field at their light cylinder, compared with what is available for millisecond pulsars, encouraged us to implement a long-term observational program for pulsars in the Northern Hemisphere, both to search for new pulsars with GRPs and to monitor known pulsars with GRPs.

Here we present some recent results of this search and monitoring program of GRPs that have been undertaken with the Large Phased Array (LPA) in 2011–2017. These results were reported for the first time at the All-Russian Astronomical Conference (VAK-2017). A review of the “Stars and Interstellar Medium” section of the conference can be found in Samus & Li (2018).

## 2 OBSERVATIONS AND DATA REDUCTION

The observations were carried out in 2011–2017 using the 1st (one beam) configuration of the LPA transit radio telescope of Pushchino Radio Astronomy Observatory (Astro Space Center, Lebedev Physical Institute). The telescope has an effective area in the zenith direction of about  $20\,000 \pm 1300 \text{ m}^2$ . One linear polarization was used. A 512-channel digital receiver with synthesized channels, each with bandwidth  $\Delta f = 5 \text{ kHz}$ , was employed. The full bandwidth of observations was 2.3 MHz (460 frequency channels were used) and was reduced by

**Table 1** List of Pulsars with GRPs

Pulsar name (epoch 2000 and 1950)	Period [s]	Frequency [MHz]	$B_{LC}$ [G]	First published
J0034-0721 (B0031-07)	0.9429	40	7.02	Kuzmin et al. (2004)
J0218+4232	0.0023	610	$31.21 \times 10^5$	Joshi et al. (2004)
J0304+1932 (B0301+19)	1.3876	111	4.76	Kazantsev et al. (2017)
J0534+2200 (B0531+21)	0.0331	40–8300	$9.8 \times 10^5$	Staelin & Reifenstein (1968)
J0529-6652*	1.0249	610	39.7	Crawford et al. (2013)
J0540-6919*	0.0505	1390	$3.62 \times 10^5$	Johnston & Romani (2003)
J0659+1414 (B0656+14)	0.3849	111	766	Kuzmin & Ershov (2006)
J0953+0755 (B0950+08)	0.2530	111	141	Singal (2001)
J1115+5030 (B1112+50)	1.6564	111	4.24	Ershov & Kuzmin (2003)
J1136+1551 (B1133+16)	1.1879	111	1.19	Kazantsev & Potapov (2015b)
J1239+2453 (B1237+25)	1.3824	111	4.14	Kazantsev & Potapov (2015a)
J1752+2359	0.4091	111	71.1	Ershov & Kuzmin (2006)
J1824-2452A	0.0030	1510	$7.41 \times 10^5$	Johnston & Romani (2003)
J1823-3021A	0.0054	685	$2.52 \times 10^5$	Knight et al. (2005)
J1939+2134 (B1937+21)	0.0016	111–5500	$1.02 \times 10^6$	Wolszczan et al. (1984)
J1959+2048	0.0016	610	$3.76 \times 10^5$	Joshi et al. (2004)

Notes: Period of a pulsar is expressed as four digits after the decimal.  $B_{LC}$  is the magnetic field at the light cylinder in Gauss. \* Pulsars in the LMC.

amplitude-frequency response of the analog receiver. The main frequency of the observations was 111 MHz. The sampling interval was 1.2288 ms for the majority of observations, and several observation sessions were carried out with sampling of 2.4576 ms. The duration of an observation session was taken equal to the time of passage for the pulsar through 0.5 of the antenna beam and depended on the declination of a given pulsar; typically this was between 3 and 10 min (about 3.5 min for PSR B1237+25 and about 11 min for PSR B0809+74, for example). All observations were carried out in individual pulses mode of the digital receiver (a sequence of individual pulses from a pulsar were recorded).

During data acquisition, phased analog signal from the radio telescope’s dipoles was sent to the receiver. In this process, a synchronizer generates trigger pulses that synchronize the operation of the digital receiver with the period of a given pulsar. Precise timing is provided by signals from the Global Positioning System (GPS). The accuracy of converting GPS time to the universal time scale is  $\pm 100$  ns. The accuracy of setting the start time of the receiver by the synchronizer is  $\pm 10$  ns, which far exceeds any reasonable requirements for accuracy of observations at a frequency of 111 MHz. For each trigger pulse, the signal is digitized at a frequency of 5 MHz and accumulates in the receiver’s buffer. These readings from the buffer are loaded into the fast Fourier transform hardware processor. Digitization of the input signal and filling of the buffer are conducted continuously without interruptions in time. Thus, continuous generation of input

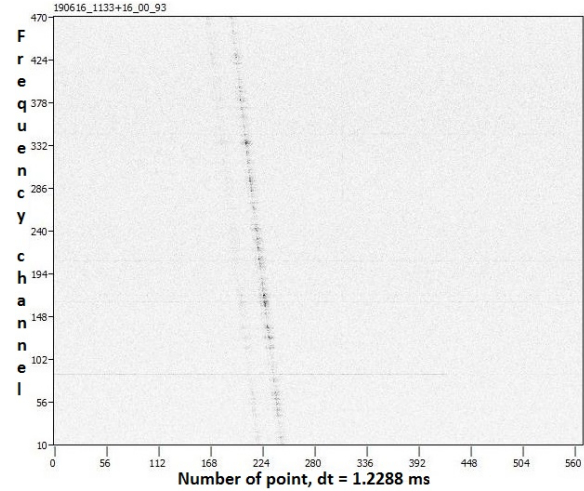


**Fig. 1** Example of a dynamical spectrum corresponding to an individual pulse from B1133+16 in 512 digitally synthesized frequency channels with uncompensated dispersion delay.

signal spectra is made, each of which contains 512 spectral channels.

A resulting file for an observation in the individual pulses mode consists of a header and array of time-series spectra. Data of time-series spectra are recorded as 32-bit floating-point numbers. So, the data take the form of a 3D array: frequency (in the frame of the receiver’s bandwidth), point (time) and intensity (in analog-to-digital converter (ADC) units). A plot of individual pulse data in frequency-time coordinates clearly demonstrates dispersion delay of a pulsar’s pulse (see Fig. 1). For every pulse, the dispersion delay was compensated off-line.

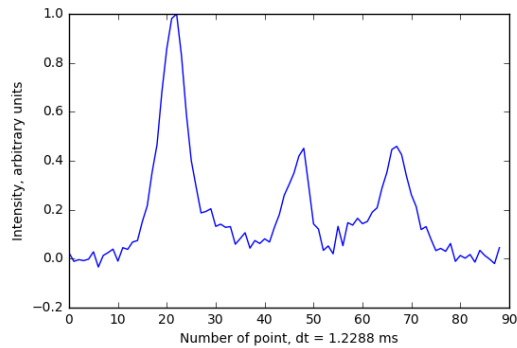


**Fig. 2** Average pulse profile of B1237+25.

As a rule, such a procedure effectively eliminates impulse interference from artificial sources. In this way, sequences of individual pulses, compensated by dispersion measure (DM) at the frequency of 111 MHz, were collected as primary information for subsequent analysis.

### 3 DATA ANALYSIS

Data in the form of sequences of individual pulses were used to generate a dynamical average pulse profile (average pulse profile per one observation session). Longitudes of an average pulse profile and off-pulse region were determined by correlation with a pattern average pulse profile of every pulsar (see Fig. 2 and 3). Off-pulse region was used to calculate background noise  $\sigma_{\text{noise}}$ . Then, pulses with a phase on a longitude of an average pulse profile of pulsar and a peak flux density of more than  $4\sigma_{\text{noise}}$  were collected. For each pulse, intensity in ADC units, intensity in peak flux density of a dynamical average pulse profile and phase in sample points were calculated. All data which satisfied the aforementioned conditions were combined into one data array. The resulting data were adjusted for the telescope's beam shape both for azimuth and zenith distances. Then we searched for the strongest pulses with peak flux density more than  $30S_{\text{avg}}$  (peak flux density of a dynamical average pulse profile of a pulsar). Data were calibrated using a noise signal (noise step) with a temperature of 2100 K injected into the receiver tract before the amplifier, which enables estimating the flux density in Jy as  $S = 2kT/A_{\text{eff}}$ , where  $S$  is the peak flux density,  $T$  is the source brightness temperature and  $A_{\text{eff}} = 20\,000 \pm 1300\text{ m}^2$  is the effective area of the 1st configuration of LPA. Such a procedure gives an estimate of the total root mean square (rms) uncertainty in absolute flux density units of about 18% (Kazantsev & Potapov 2017). For pulsars B0329+54 and B1133+16, the aver-

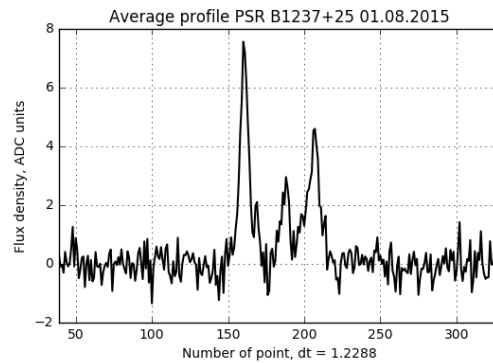


**Fig. 3** Dynamical average pulse profile of B1237+25.

aged value for system temperature during observation (5 K for ADC unit) was taken due to a shortage of calibration data, therefore further evaluation of their peak flux density in Jy should be mentioned as an upper limit. Finally, a statistical analysis of pulse distributions in absolute (in Jy) and in  $S_{\text{avg}}$  per session units was made for pulsars with GRPs to confirm the statistical (power-law) criterion.

## 4 RESULTS

### 4.1 Pulsars without GRPs

As is well known, the overwhelming majority of pulsars does not generate GRPs. Nevertheless, it was interesting for us to obtain statistics for a set of such pulsars to compare with those of pulsars with GRPs. This sub-section includes data on three observed pulsars which did not demonstrate GRPs or giant-like pulses. These pulsars are referred to later as “regular” radio pulsars.

#### 4.1.1 B0320+39 (J0332+5434)

B0320+39 is a slowly rotating pulsar in the Northern Hemisphere. This pulsar has a two-component average profile at 111 MHz. The occurrence of giant pulses from this pulsar has not been reported. There were 9406 pulses that were detected and analyzed which satisfied the conditions stated in Section 3. The strongest observed pulse is 29 times larger than the dynamical average pulse profile (see Fig. 4(a)) and has width 1/4 as narrow as an average pulse at 10% of the average pulse peak flux density and about 1/2 of the relevant component at 50%. Figure 5(a) shows that the strong pulse is very prominent among regular pulses. The distribution shown in its pulse intensity histogram (see Fig. 6(a), 8(a)) has a form close to a simple log-normal (power-law) distribution.

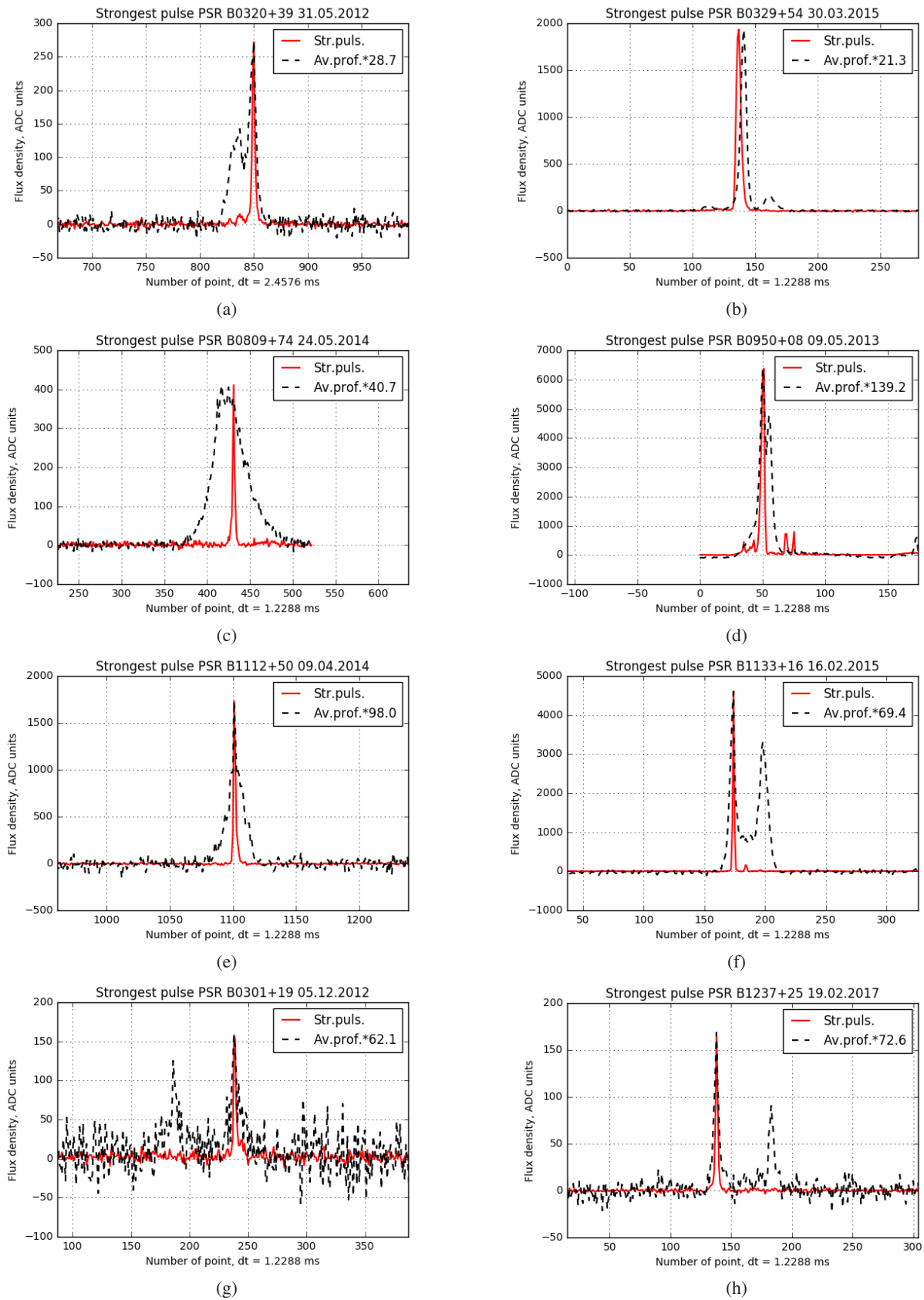
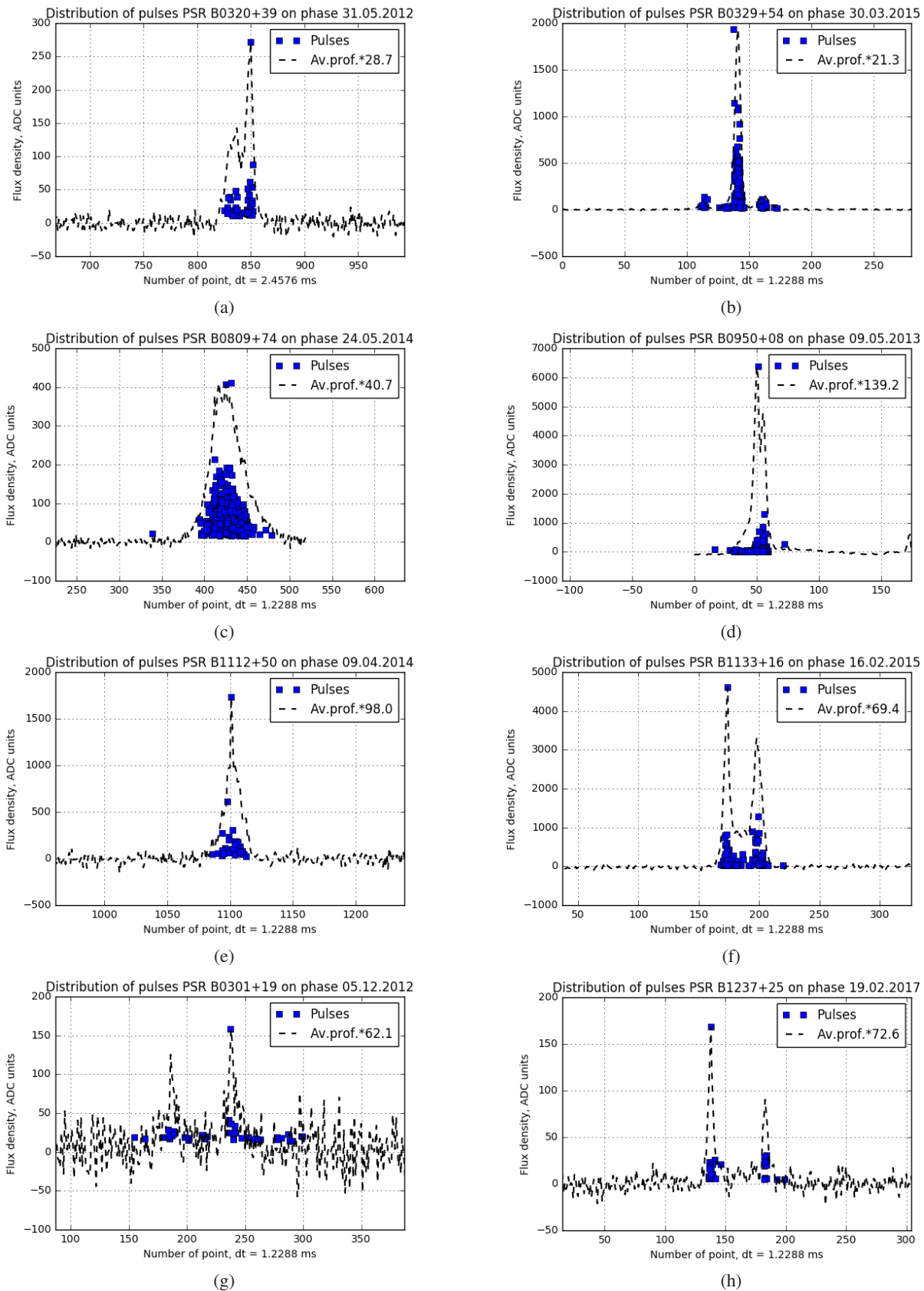
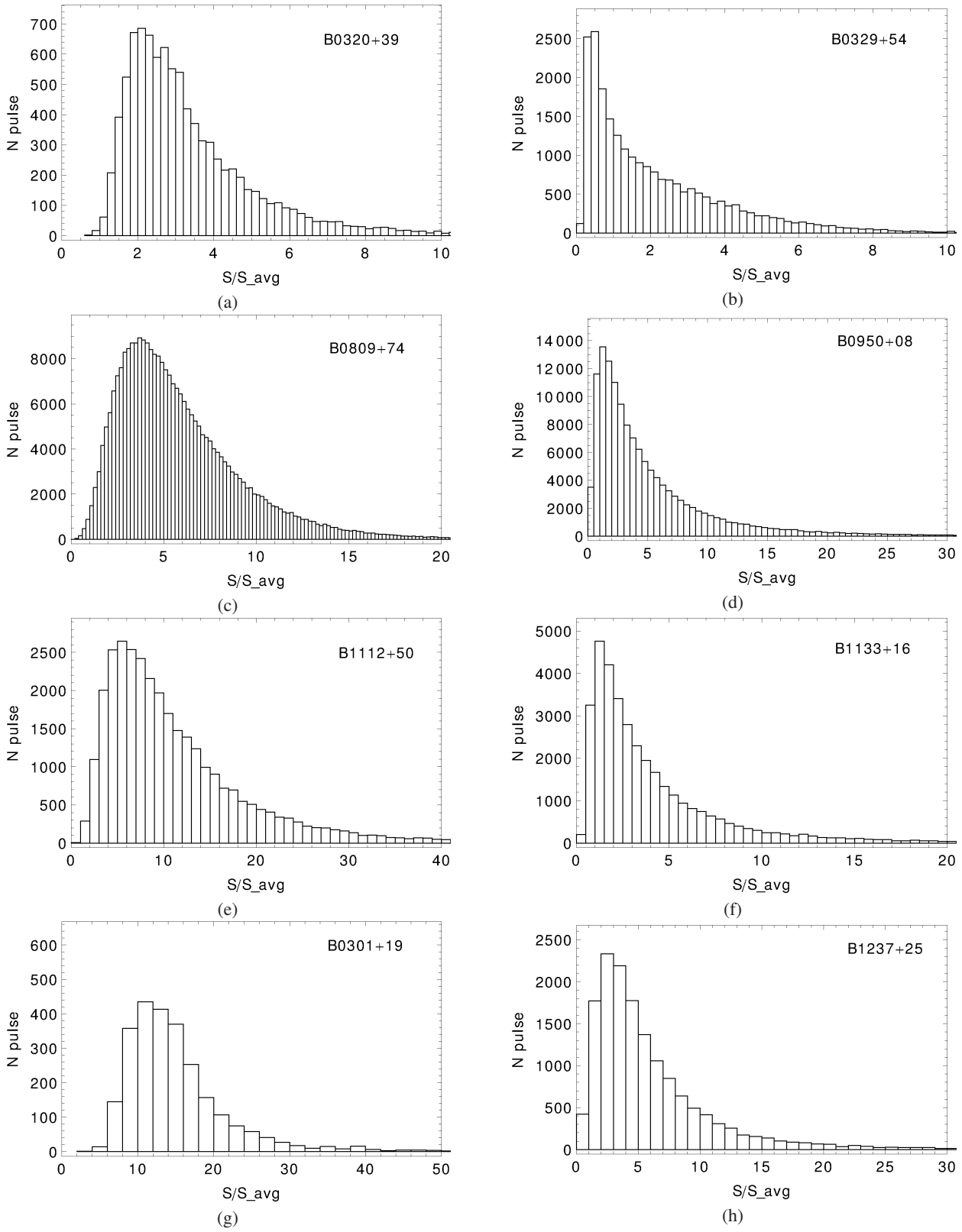


Fig. 4 The strongest individual pulse in an observation session is shown with an increased dynamical average profile.



**Fig. 5** The distribution of individual pulses from a pulsar in an observation session is shown with an increased dynamical average profile.



**Fig. 6** Pulse intensity histogram at 111 MHz for a pulsar in  $S_{\text{avg}}$  units.

**Table 2** Information About Observations for Each Pulsar. DM Denotes Dispersion Measure of the Interstellar Medium in the Direction of a Given Pulsar

No.	Name of pulsar epoch 1950(2000)	Period [s]	DM [pc cm <sup>-3</sup> ]	Number of observ. sessions	Total time of data folding [h]
1	B0301+19 (J0304+1932)	1.3876	15.66	275	15.47
2	B0320+39 (J0323+3944)	3.0321	26.19	155	10.70
3	B0329+54 (J0332+5434)	0.7145	26.76	63	5.80
4	B0809+74 (J0814+7429)	1.2922	5.75	588	116.72
5	B0950+08 (J0953+0755)	0.2531	2.97	677	36.40
6	B1112+50 (J1115+5030)	1.6564	9.19	1063	89.01
7	B1133+16 (J1136+1551)	1.1879	4.84	616	33.94
8	B1237+25 (J1239+2453)	1.3824	9.25	568	33.37

**Table 3** Peak Flux Density Distribution of GRPs and Strongest Individual Pulses Observed

No	BName	$\alpha$	Max pulse [ $S_{\text{avg}}$ ]	Max pulse [Jy] ***
1	B0320+39	–	28.7	196
2	B0329+54	–	21.3	1680 *
3	B0809+74	–	40.7	2680
1	B0301+19	$-2.32 \pm 0.17$	106.5	687
2	B0950+08	$-1.93 \pm 0.03$	142.1	16800
3	B1112+50	$-2.86 \pm 0.11$	206.5	1490
4	B1133+16	$-1.28 \pm 0.04 / -2.78 \pm 0.06$ **	86.7	5030 *
5	B1237+25	$-2.14 \pm 0.05$	108.5	1350

Notes:  $\alpha$  is the exponent of the power function of distribution of the absolute peak flux density (the slope of the straight line in Log-Log scale). \* An upper limit due to the shortage of calibration data – see Section 3 for explanation. \*\* Exponents of the first and second components of distribution function (see Fig. 8(f)). \*\*\* Uncertainty is  $\sim 18\%$  for all flux estimations.

#### 4.1.2 B0329+54 (J0332+5434)

B0329+54 is one of the brightest isolated pulsars, and possibly has a planetary system (Shabanova 1995), see Starovoit & Rodin (2017) for discussion. As in the case of B0320+39, there were no detected GRPs or anomalous pulses for this pulsar. We analyzed 22 874 individual pulses which satisfied the conditions. No pulses were found with peak flux density exceeding the dynamical average profile by more than 30 times. One of the strongest observed pulses is shown in Figure 4(b). As can be seen from the figure, the powerful pulse has comparable duration with a main component of the average profile of the pulsar and is shifted to its leading edge. In spite of the absence of GRPs, distributions of the flux density, both in peak flux density and relative to dynamical average profile units, are quite complicated and cannot be described with a simple log-normal model, see Figures 7 and 8.

#### 4.1.3 B0809+74 (J0814+7429)

Because of the high declination of this pulsar, duration of one observation session with LPA was the longest and equal to about 11 min. This allowed us to detect

281 331 individual pulses from this pulsar which satisfied our conditions. So many pulses make this research the most voluminous for this pulsar. Forty-nine pulses with peak flux density exceeding the peak flux density of the dynamical average profile by more than  $30S_{\text{avg}}$  were observed. Figure 4(c) shows an example of one strong pulse. For the first time, similar pulses were observed at 18–40 MHz (Ulyanov et al. 2006) and were named anomalously strong pulses. The pulsar has a distinct drifting sub-pulse phenomenon (Page, 1973) which leads to a tangible “smudging” of peak flux density in the average profile. Distributions, both in peak flux density and in units of  $S_{\text{avg}}$  for pulses with flux  $> 15S_{\text{avg}}$ , show a combined distribution with a power-law part that is not strong enough to classify pulses as GRPs.

## 4.2 “Old” Pulsars with GRPs

This group includes pulsars that display the phenomenon of GRP generation which were discovered earlier outside our observational program. For these objects, a comparative analysis of statistical distribution was done. It should be noted that the discoveries and observations were carried out at 103–180 MHz, which facilitates comparative analysis with the associated statistics.

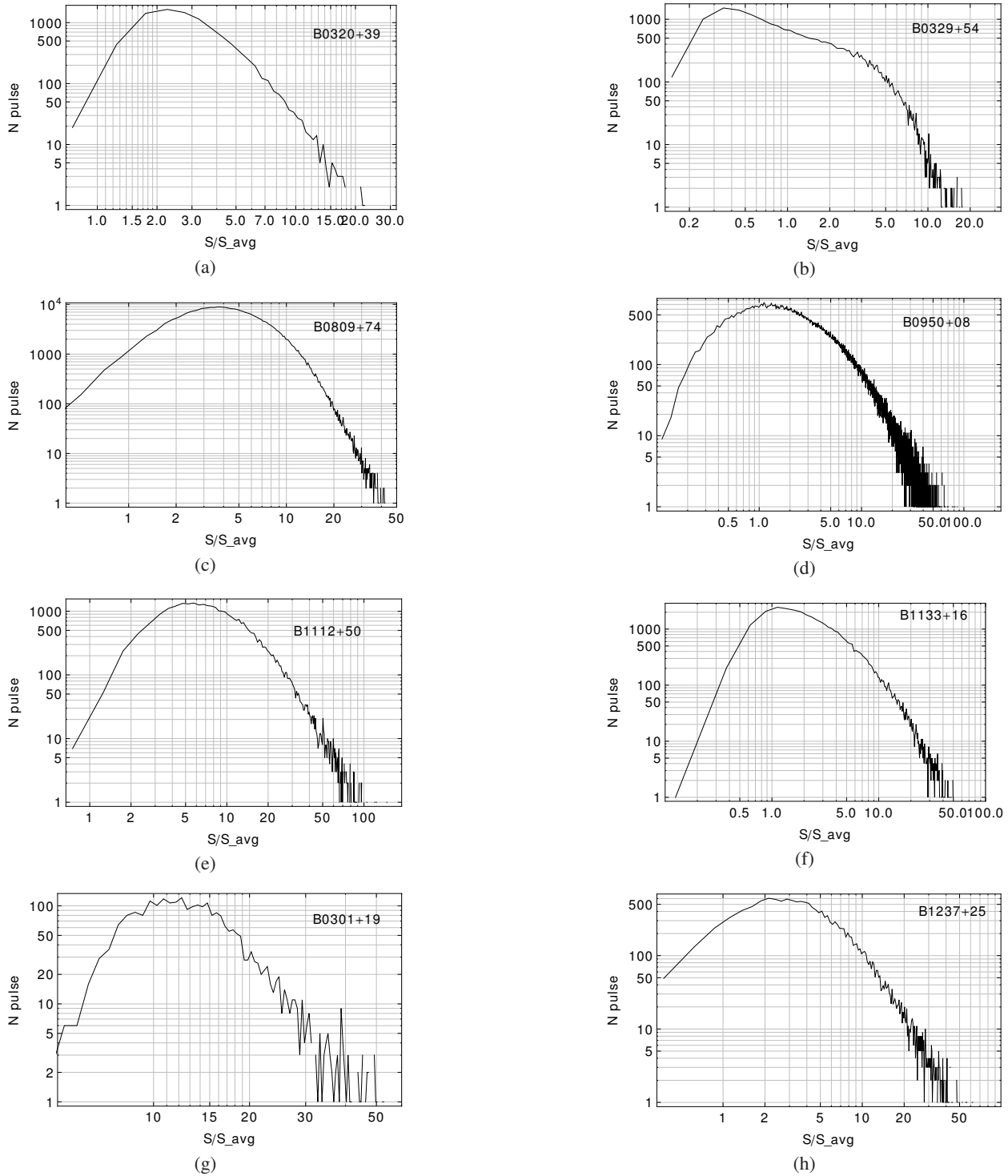


**Fig. 7** The distribution of peak flux densities from individual pulses in  $S_{avg}$  units.

#### 4.2.1 B0950+08 (J0953+0755)

For the first time, GRPs from this pulsar were discovered by Singal (2001) at 103 MHz. The value of  $20S_{avg}$  was taken in Singal (2001) as the threshold for pulses to be

called giant. Under this approach, roughly one percent of about one million pulses from B0950+08 were classified as GRPs. We analyzed 155 834 individual pulses from this pulsar and detected 3422 pulses that showed more than  $20S_{avg}$  (and 1062 pulses more than  $30S_{avg}$ ),

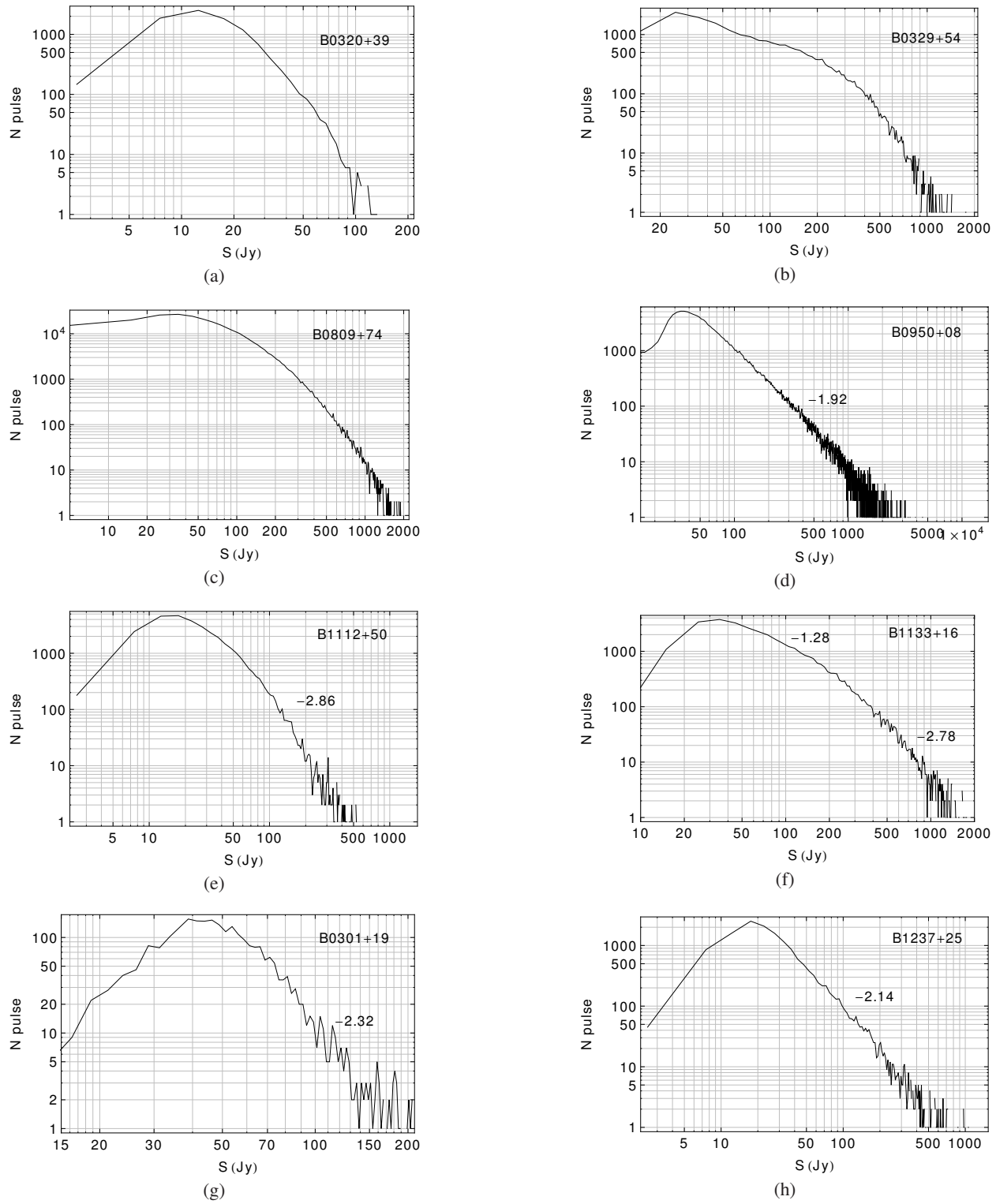


**Fig. 8** The distribution of peak flux densities from individual pulses in absolute (Jy) units.

representing 2.2 (0.68) percent of pulses with more than  $4\sigma_{\text{noise}}$  in terms of peak flux. Observations of giant pulses from the pulsar were carried out using LPA by

Smirnova (2012) earlier. The strongest individual pulses in the papers cited above were 300 and 508 times as strong as an average profile, respectively. In the frame of

the present work, the strongest pulse in  $139.2S_{\text{avg}}$  was detected and is shown in Figure 4(d). Notable tertiary peaks are interference. At the same time, the strongest pulse detected during our observational program has a peak flux density of 16.8 kJy, which is the strongest value ever detected for this pulsar (a pulse as strong as 15.2 kJy was detected earlier in Smirnova 2012). It is worth noting that the distribution of GRPs in our work (Fig. 8(d)) differs significantly from the two-component distribution found in Smirnova (2012), which can be explained by instability of the distribution based on relatively short duration of time.

#### 4.2.2 B1112+50 (J1115+5030)

Ershov & Kuzmin (2003) reported about GRPs from this pulsar at a frequency of 111 MHz. In 105 observation sessions, 126 GRPs were detected in cited work. This represents about 0.67 percent of the full quantity of the pulsar’s periods. In our research, this ratio is equal to 0.83 percent. The duration and localization of GRPs are consistent in both works. Sometimes, observed GRPs have a complex form which can be formed by a microstructure that cannot be resolved at low radio frequencies. Figure 4(e) shows one of the giant pulses in comparison with the increased dynamical average pulse profile. Distribution in absolute peak flux density demonstrates power-law behavior with exponent  $\alpha = -2.86$ , which differs from the earlier result of Ershov & Kuzmin (2003) with  $\alpha = -3.6$ .

#### 4.2.3 B1133+16 (J1136+1551)

Bright pulses from this pulsar were noted earlier in Kramer et al. (2003) at 5 GHz, but it was identified as a possible source of giant pulses by Karuppusamy & Stappers (2008) and Kazantsev & Potapov (2015b). We analyzed 58 642 individual pulses from pulsar B1133+16 and detected 153 pulses more than  $30S_{\text{avg}}$ . This pulsar has an average profile with two well separated components. GRPs were detected in both. An example of observed giant pulses and the increased dynamical average profile are shown in Figure 4(f). The pulse has extremely short duration in comparison with the relevant component average profile of this pulsar (unresolved at the sampling interval of 1.2288 ms at 50% of intensity). The distribution of pulses is quite complicated and may represent strong pulses corresponding to a two-component power-law distribution (Fig. 8(f)) with a bend near 250 Jy.

### 4.3 “Fresh” Pulsars with GRPs

This sub-section describes newly identified pulsars with GRPs which were discovered in the frame of our search program with LPA at 111 MHz.

#### 4.3.1 B0301+19 (J0304+1932)

For the first time, existence of GRPs from this pulsar was reported by Kazantsev et al. (2017). Our previous research included a small amount of observation sessions. Only 884 pulses with peak flux density more than  $3\sigma_{\text{noise}}$  were analyzed. In the present work, the sample of 3160 individual pulses of a pulsar which were more than  $4\sigma_{\text{noise}}$  by amplitude was obtained and processed. Eighty pulses which can be classified as giant were detected. B0301+19 is a sufficiently weak pulsar and its dynamical average profile is faint except at the time the GRPs were generated, when the average profile becomes more detectable.

#### 4.3.2 B1237+25 (J1239+2453)

The first report about GRPs from B1237+25 was published in Kazantsev & Potapov (2015a), but more detailed statistical analysis was made by Kazantsev & Potapov (2017). One example of an observed GRP is shown in Figure 4(h). The sample used for statistical analysis was increased by about two times and includes 22 207 pulses which are more than  $4\sigma_{\text{noise}}$  by amplitude; 168 pulses with intensity more than  $30S_{\text{avg}}$  were detected. The peak flux distribution in Fig. 8(h) demonstrates a clear one-component distribution that differs from a two-component distribution obtained in our earlier research, both in terms of power and form.

## 5 DISCUSSION AND CONCLUSIONS

Long-term observations of 71 pulsars in the Northern Hemisphere were carried out at 111 MHz with LPA in order to search for GRPs. The analysis of fluctuations in the pulses’ intensity from B0320+39 and B0329+54 has led to an absence of pulses which can be classified as giant. Pulses’ peak flux density distributions, both in terms of  $S_{\text{avg}}$  and absolute units (Jy), do not demonstrate a clear bimodal form that is generally thought to be typical for pulsars with GRPs. Nevertheless, the distribution for B0329+54 has a complicated form that cannot be described by a simple log-normal distribution.

Anomalously strong pulses from B0809+74 were discovered at 111 MHz. These pulses form a qualitatively

significant power-law tail in peak flux density distribution by  $S_{\text{avg}}$ .

Generation of GRPs from B0301+19, B0950+08, B1112+50, B1133+16 and B1237+25 was confirmed. The statistical distributions of pulses from long-term observations were plotted for these pulsars. These distributions normally have a bimodal form: power-law for strong pulses and log-normal for regular pulses.

It is not surprising that forms of pulse intensity histograms at 111 MHz (Fig. 6) differ from the corresponding histograms at 2695 MHz for a pulsar with GRPs (see Hesse & Wielebinski 1974). This fact may be explained by instability in the radio emission of active pulsars in time. The difference between the histogram at 111 MHz and that at 2695 MHz for a highly stable pulsar without GRPs – B0329+54 – is much more interesting and probably may be related to the distinction between generation of radio emission at low and high frequencies.

It is worth noting that in general we cannot see quite strict qualitative differences between distributions of “regular” pulsars and pulsars with GRPs. On the contrary, it is typical to see a “zoo” of distributions with quite complicated forms that gradually change from one (“regular”) class of pulses to another (GRPs). This is a consequence of the fact that our statistical criterion is not so robust in the case of GRPs generated by pulsars with low magnetic field at their light cylinder and should be used with caution to classify GRPs. Moreover, sporadic generation of strong pulses in the dataset of such pulsars as B0329+54 and B0809+74 together with their complex and asymmetrical distribution may be caused by the fact that some amount of pulses is generated by the same physical mechanism as GRPs, and that this phenomenon is much more typical for pulsars than was supposed earlier.

**Acknowledgements** We thank S.V. Logvinenko for technical support during the observations and V.V. Oreshko and S.A. Tyulbashev for useful discussion. This work was supported in part by the Program of the Presidium of Russian Academy of Sciences “Non-stationary processes in the Universe.”

## References

- Cognard, I., Shrauner, J. A., Taylor, J. H., & Thorsett, S. E. 1996, *ApJ*, 457, L81
- Crawford, F., Altemose, D., Li, H., & Lorimer, D. R. 2013, *ApJ*, 762, 97
- Ershov, A. A., & Kuzmin, A. D. 2003, *Astronomy Letters*, 29, 91
- Ershov, A. A., & Kuzmin, A. D. 2006, *Chinese Journal of Astronomy and Astrophysics Supplement*, 6, 30
- Hankins, T. H., & Eilek, J. A. 2007, *ApJ*, 670, 693
- Hesse, K. H., & Wielebinski, R. 1974, *A&A*, 31, 409
- Johnston, S., & Romani, R. W. 2003, *ApJ*, 590, L95
- Joshi, B. C., Kramer, M., Lyne, A. G., McLaughlin, M. A., & Stairs, I. H. 2004, in *IAU Symposium*, 218, *Young Neutron Stars and Their Environments*, ed. F. Camilo & B. M. Gaensler, 319
- Karuppusamy, R., & Stappers, B. W. 2008, in *American Institute of Physics Conference Series*, 983, *40 Years of Pulsars: Millisecond Pulsars, Magnetars and More*, ed. C. Bassa, Z. Wang, A. Cumming, & V. M. Kaspi, 121
- Kazantsev, A. N., & Potapov, V. A. 2015a, *Astronomicheskij Tsirkulyar*, 1620, 1
- Kazantsev, A. N., & Potapov, V. A. 2017, *Astronomy Reports*, 61, 747
- Kazantsev, A. N., Potapov, V. A., & Safronov, G. B. 2017, *Astronomicheskij Tsirkulyar*, 1638, 1
- Kazantsev, N. A., & Potapov, V. A. 2015b, *Astronomicheskij Tsirkulyar*, 1628, 1
- Knight, H. S., Bailes, M., Manchester, R. N., & Ord, S. M. 2005, *ApJ*, 625, 951
- Kramer, M., Karastergiou, A., Gupta, Y., et al. 2003, *A&A*, 407, 655
- Kuzmin, A. D., & Ershov, A. A. 2006, *Astronomy Letters*, 32, 583
- Kuzmin, A. D., Ershov, A. A., & Losovsky, B. Y. 2004, *Astronomy Letters*, 30, 247
- Page, C. G. 1973, *MNRAS*, 163, 29
- Petrova, S. A. 2006, *Chinese Journal of Astronomy and Astrophysics Supplement*, 6, 113
- Ritchings, R. T. 1976, *MNRAS*, 176, 249
- Romani, R. W., & Johnston, S. 2001, *ApJ*, 557, L93
- Samus, N. N., & Li, Y., *RAA (Research in Astronomy and Astrophysics)*, 2018, 18, 88
- Shabanova, T. V. 1995, *ApJ*, 453, 779
- Singal, A. K. 2001, *Ap&SS*, 278, 61
- Smirnova, T. V. 2012, *Astronomy Reports*, 56, 430
- Staelin, D. H., & Reifenstein, III, E. C. 1968, *Science*, 162, 1481
- Starovoit, E. D., & Rodin, A. E. 2017, *Astronomy Reports*, 61, 948
- Sutton, J. M., Staelin, D. H., & Price, R. M. 1971, in *IAU Symposium*, 46, *The Crab Nebula*, ed. R. D. Davies & F. Graham-Smith, 97
- Taylor, J. H., & Huguenin, G. R. 1971, *ApJ*, 167, 273
- Ulyanov, O. M., Zakharenko, V. V., Konovalenko, O. O., et al. 2006, *Russian Radio Physics and Radio Astronomy*, 11, 113
- Wolszczan, A., Cordes, J. M., & Stinebring, D. R. 1984, in *Millisecond Pulsars*, 63